ARTICLE

doi:10.1038/nature09403

Ocean nutrient ratios governed by plankton biogeography

Thomas S. Weber[1] & Curtis Deutsch[1]

The major nutrients nitrate and phosphate have one of the strongest correlations in the sea, with a slope similar to the average nitrogen (N) to phosphorus (P) content of plankton biomass (N/P = 16:1). The processes through which this global relationship emerges despite the wide range of N/P ratios at the organism level are not known. Here we use an ocean circulation model and observed nutrient distributions to show that the N/P ratio of biological nutrient removal varies across latitude in Southern Ocean surface waters, from 12:1 in the polar ocean to 20:1 in the sub-Antarctic zone. These variations are governed by regional differences in the species composition of the plankton community. The covariation of dissolved nitrate and phosphate is maintained by ocean circulation, which mixes the shallow subsurface nutrients between distinct biogeographic provinces. Climate-driven shifts in these marine biomes may alter the mean N/P ratio and the associated carbon export by Southern Ocean ecosystems.

The oceanic cycles of life's essential elements—carbon, nitrogen and phosphorus—are closely coupled through the metabolic requirements of phytoplankton, whose average proportions of these elements, C/N/P = 106:16:1, are known as the Redfield ratios[1–3]. The similarity between the average N/P ratio of plankton biomass and spatial variations of dissolved nitrate (NO_3^-) and phosphate (PO_4^{3-}) has long been taken to imply that a relatively constant number of N atoms per atom of P are assimilated by phytoplankton throughout the surface ocean and released by the respiration of organic matter at depth[4,5]. The Redfield N/P ratio is therefore viewed as a critical threshold between the N-limitation and P-limitation of marine photosynthesis and the carbon it sequesters[6,7]. On millennial timescales, the global oceanic reservoirs of N and P are thought to be maintained near the Redfield ratio by species that add N to the ocean through biological N_2 fixation when N is limiting but are out-competed by other plankton when it is not[8]. The Redfield ratio thus underpins the geochemical understanding of species competition and coexistence and the long-term regulation of ocean fertility and carbon storage.

The N/P ratios observed in marine phytoplankton span at least an order of magnitude[9] and vary at two distinct levels of biological organization: phylogenetic differences between species and larger taxonomic groups[10], and phenotypic variability between populations of the same species that are acclimated to different physical or chemical environments[11]. The Redfield ratio of N/P = 16:1 thus has no biological basis apart from being an approximate average across a wide range of species and environmental conditions[3,12].

To reconcile the biological and geochemical perspectives on Redfield N/P ratios, some process is required to effectively average out the wide variations in N/P at the organism level (N/P_{org}) and maintain the covariation of NO_3^- and PO_4^{3-} observed in sea water. Two such mechanisms can be proposed. On the one hand, the local balance of species and phenotypes and their seasonal succession may average deviations from Redfield stoichiometry over small spatial scales within the plankton ecosystem. This process, referred to here as ecosystem averaging, would lead to the export of organic matter from the surface with a relatively uniform N/P ratio (N/P_{exp}) of ~16:1, consistent with the current view. On the other hand, N/P_{exp} may vary between marine biomes owing to sustained regional differences in the physiological state or species composition of the plankton community. The tight correlation between NO_3^- and PO_4^{3-} could still be achieved, however, if circulation and mixing in the ocean interior were to effectively integrate the nutrients exported and remineralized from regions both above and below the Redfield ratio, a mechanism we refer to as circulation averaging.

Southern Ocean export ratios

These two hypotheses cannot be directly assessed from the composition of sinking organic matter, owing to the sparse spatial and temporal resolution of those observations[9]. However, they can be distinguished on the basis of their effects on the distributions of dissolved NO_3^- and PO_4^{3-} in the upper ocean. In the case of ecosystem averaging, the biological removal and subsequent remineralization of nutrients at the Redfield ratio would conserve the tracer N* ($N^* = [NO_3^-] - 16[PO_4^{3-}]$, where square brackets denote concentration) along the transport path of a water parcel[13]. The only sources of variation in N* would be addition of nitrate through N_2 fixation or atmospheric N deposition, and nitrate removal through anaerobic denitrification[13]. In the case of circulation averaging, regions of high N/P uptake at the surface would cause N* to decrease along flow lines, whereas regions with low uptake ratios would increase N*. To detect changes in N* that are caused by stoichiometric variability of plankton, rather than sources or sinks of fixed N, we focus on the Southern Ocean poleward of latitude 35° S. Here N_2 fixation is virtually excluded by the abundance of dissolved NO_3^- and low iron concentrations[14], terrestrial N sources to the atmosphere are remote[15] and high O_2 concentrations inhibit denitrification[16]. We also restrict our analysis to the open ocean north of 70° S, where over 100,000 measurements of NO_3^- and PO_4^{3-} concentrations are widely distributed throughout the water column[17].

In the Southern Ocean, physical and chemical properties are efficiently communicated between ocean basins by rapid circumpolar currents, so the largest hydrographic gradients are across latitude[18]. There is no systematic zonal variation of N* in this region, but its zonal mean values show pronounced gradients along pathways of the large-scale meridional overturning circulation (Fig. 1a). In the

[1]Department of Atmospheric and Oceanic Sciences, University of California Los Angeles, Los Angeles, California 90095, USA.

©2010 Macmillan Publishers Limited. All rights reserved

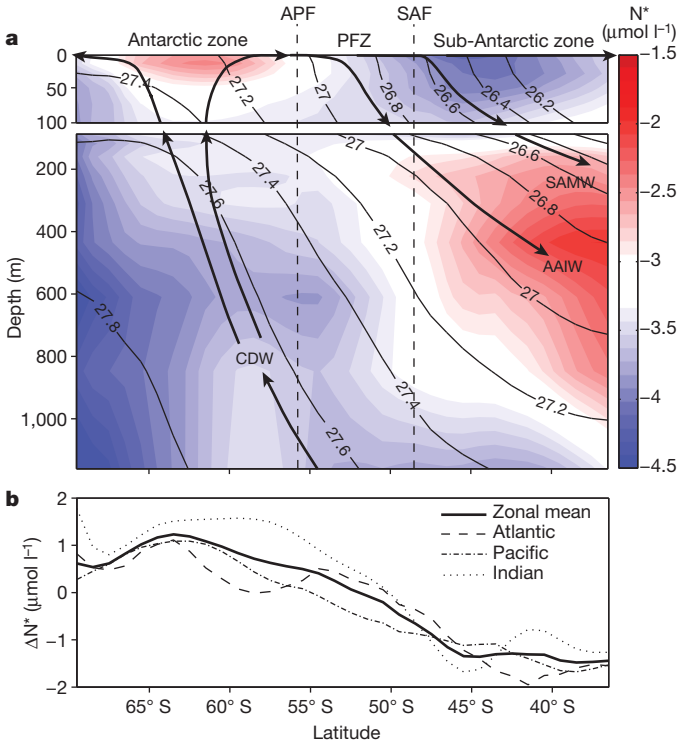

Figure 1 | Observed N* distribution in the Southern Ocean. **a**, Zonal mean section of N* ($[NO_3^-] - 16[PO_4^{3-}]$), with potential density anomaly contours ($\rho_\theta - 1{,}000\,kg\,m^{-3}$; thin lines) and schematic large-scale meridional overturning circulation patterns (arrows). Upwelling circumpolar deep water (CDW) is driven across the Antarctic polar front (APF) and the sub-Antarctic front (SAF) by Ekman transport, and subsides in the polar frontal zone (PFZ) to form Antarctic intermediate water (AAIW) and sub-Antarctic mode water (SAMW). **b**, Zonal mean vertical difference in N* between the surface and the thermocline ($\Delta N^* = N^*_{0-75\,m} - N^*_{200-800\,m}$), globally and in individual sectors of the Southern Ocean.

Antarctic zone, N* is higher at the surface than in the circumpolar deep water upwelling from depth. As these high-N* surface waters are driven northwards across the Antarctic polar front and the sub-Antarctic front by westerly winds, they become depleted in NO_3^- relative to PO_4^{3-}, reducing N* by $\sim 2\,\mu mol\,l^{-1}$ between 65° S and 40° S. In the deeper waters, from which nutrients are entrained into the surface during winter mixing, the opposite gradient is observed: N* increases towards the north. Consequently, the vertical difference in N* between the surface and thermocline ($\Delta N^* = N^*_{0-75\,m} - N^*_{200-800\,m}$) reverses sign from positive in the Antarctic zone to negative in the sub-Antarctic (Fig. 1b). This trend is independently observed in the Pacific, Atlantic and Indian sectors of the Southern Ocean, indicating that the zonal mean N* gradients are robust.

The compatibility of these observations with the hypothesis of ecosystem averaging can be tested by predicting nutrient distributions under the assumption that uptake and remineralization occur universally at the Redfield N/P ratio (model 1; see Methods Summary). We simulate the physical transport and biological cycling of nutrients in an ocean circulation model, using climatological NO_3^- and PO_4^{3-} concentrations throughout the water column at the northern boundary (35° S). In this simulation, the rate of biological PO_4^{3-} export is diagnosed by damping surface concentrations towards their observed values, and NO_3^- is removed at a fixed ratio to PO_4^{3-} of 16:1. The exported nutrients are then remineralized as they sink through the water column. Predicted export production rates are 10–100 mmol P $m^{-2}\,yr^{-1}$, with a peak at ~50° S, in good agreement with other model and data-derived estimates[19]. However, the predicted surface N* gradient increases northwards from $-4\,\mu mol\,l^{-1}$ in the Antarctic zone to $-2.5\,\mu mol\,l^{-1}$ in the sub-Antarctic, and there is

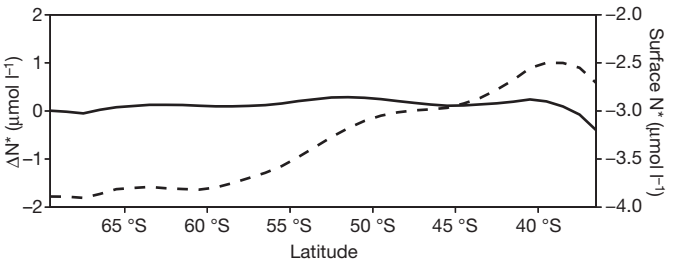

Figure 2 | Redfield N* prediction. Southern Ocean surface N* gradient (dashed line) and ΔN* (solid line) predicted in model 1, assuming nutrient uptake and remineralization at the Redfield ratio. The northward increase in surface N* and low ΔN* values are inconsistent with observations.

little variation in N* with depth (Fig. 2). This gradient reflects the isopycnal transport of N* values from the subtropical boundary into the Southern Ocean, but is inconsistent with the observations (Fig. 1a). The observed N* distribution contradicts the hypothesis of ecosystem averaging, and implies nutrient removal below the Redfield ratio polewards of ~55° S and above the Redfield ratio to the north.

To derive a quantitative picture of N/P_{exp} consistent with the nutrient observations, we conduct a second simulation (model 2; see Methods Summary) in which the export of NO_3^- and PO_4^{3-} are independently diagnosed south of 35° S. In this simulation, nutrient supply from below the surface layer is computed using observed nutrient concentrations in the subsurface, eliminating errors that might arise from uncertainty in model remineralization rates (Supplementary Fig. 1). The basin-integrated export fluxes are 0.125 Mmol P yr^{-1} and 2.05 Mmol N yr^{-1}, yielding a basin-wide export ratio of N/P ≈ 16.5:1, nearly identical to the Redfield ratio. However, large deviations from the Redfield ratio are revealed on the regional scale, with $N/P_{exp} < 16{:}1$ throughout most of the polar ocean and $N/P_{exp} > 16{:}1$ in the sub-Antarctic (Fig. 3a), as anticipated from N*. The zonal mean export ratio varies almost twofold with latitude, increasing from 12.5 ± 2 at 60° S to 20 ± 1 at 40° S (Fig. 3b), consistent with the limited observations of nutrient drawdown ratios[20]. This meridional trend is not dependent on the choice of circulation model, the biological parameterization, the depth of net nutrient uptake or the inclusion of dissolved organic matter cycling (Supplementary Notes and Supplementary Figs 2–5). It derives from the northward decrease in surface N* and its vertical gradient along shallow pathways of the meridional overturning circulation.

Sources of N/P variability

The latitudinal variation in N/P_{exp} reflects the elemental composition of the plankton that assimilate nutrients and export them from the surface. Nutrient uptake ratios measured in algal monocultures are highly species dependent[10], suggesting that species distributions could

Table 1 | Correlation of N/P_{exp} with potential sources of variability

	Zonal ($n = 35$)	1° × 1° ($n = 11{,}408$)	Expected relationship		Ref.
			Direction	N/P range	
Community composition*	−98	−50	Negative	10–31	10
Light (mixed layer average)	62	19	Negative	7–41	11
Summertime growth rate†	86	39	Negative	8–45‡	12
[Fe]	72	22	Positive	9–14	24
Temperature	89	38	Positive	20–25	25

Zonal and 1° × 1° values are correlation coefficients ($100R^2$) from model results, with negative values indicating negative correlations. The expected direction and N/P range are obtained from culture or modelling studies that varied the property independently. The direction of the relationship is opposite to that expected for growth rate and light, and the magnitude is too large to be explained by iron concentration or temperature.
* Characterized by percentage export by diatoms.
† Estimated from nutrients, light, iron concentration and temperature (Supplementary Information).
‡ Obtained by varying allocation to reproductive machinery in cellular model.

©2010 Macmillan Publishers Limited. All rights reserved

influence N/P_{exp} on large scales in the ocean. The region from 35° S to 70° S encompasses two distinct ecological biomes, the Antarctic polar biome polewards of 55° S and the Westerly Winds biome to the north, each with characteristic plankton communities and trophic interactions[21]. Direct observations are too sparse to determine the community structure on the scales required here, but diatoms are consistently reported as a major component of Southern Ocean assemblages[22]. Diatoms are the only algal family to build silica-based frustules, so their fractional contribution to exported organic matter (ϕ_{diat}) can be diagnosed from the observed silicic-acid ($Si(OH)_4$) distribution[23] (Methods Summary). Consistent with observations[22], silica export fluxes show that diatoms account for over 80% of N export throughout the $Si(OH)_4$-replete Antarctic polar biome, and less than 20% in the $Si(OH)_4$-poor Westerly Winds biome (Fig. 3b). A strong negative correlation exists between the N/P ratio of nutrient export and the fraction of that export attributed to diatoms:

$$N/P_{exp} = 20.39 - 9.6\phi_{diat} \quad (P < 0.0001)$$

This indicates that Southern Ocean communities comprise diatoms with a low N/P ratio, of ~11:1, and a remaining population with a high average N/P ratio, of ~20. This simple characterization of the plankton community structure accounts for 50% of the spatial variance in the N/P ratio of nutrient drawdown and 98% of the variance in its zonal mean value.

We also consider a range of environmental properties that can influence N/P_{org} at the phenotypic level (Table 1 and Supplementary Methods). Cellular resources are selectively allocated to P-rich reproductive biomolecules during exponential growth[12], and N-rich protein-pigment complexes during slow growth under light limitation[11]. In diatom cultures N/P_{org} varies as a function of iron availability[24], whereas in picoplankton cultures it is moderately sensitive to temperature[25]. In all cases, the diagnosed trend in N/P_{exp} is either weakly correlated with the relevant environmental parameter or inconsistent with the direction or magnitude of its predicted effect.

These findings indicate that large-scale variability in nutrient uptake ratios stems primarily from the relative abundance of species with distinct metabolic requirements. Similar species-driven deviations from the Redfield ratio have been observed on smaller scales in the Southern Ocean[20,26]. In the coastal waters of the Ross Sea, the local balance of low-N/P diatoms and high-N/P prymnesiophytes was found to maintain an export ratio of N/P ≈ 16:1 on relatively small spatial scales[26]. In contrast, we find that the long-term biogeography of plankton communities produces regional deviations from Redfield uptake ratios across vast expanses of the open Southern Ocean.

Ocean circulation averaging

In the presence of large spatial variations in N/P_{exp}, vigorous physical mixing is needed to enforce the observed covariation between NO_3^- and PO_4^{3-} (ref. 5). To test this circulation averaging mechanism, we conduct a third simulation in which N/P_{exp} is diagnosed from surface nutrients and organic particles transmit the signature of variable plankton stoichiometry into the subsurface, where they remineralize (model 3; see Methods Summary). The predicted subsurface nutrient concentrations can be considered the sum of the accumulated product of remineralization within the Southern Ocean ($[NO_3^-]_{rem}$ and $[PO_4^{3-}]_{rem}$) and a component that is transported either from the surface waters as unutilized nutrients or from outside the Southern Ocean (Supplementary Methods).

Directly beneath the zone of net community production, $[NO_3^-]_{rem}/[PO_4^{3-}]_{rem}$ increases northwards from ~12.5:1 in the Antarctic zone to ~21:1 in the sub-Antarctic, reflecting the full range of latitudinal variability in N/P_{exp} (Fig. 4). However, within 100 m of the compensation depth mixing has reduced this variability by >50%, and below 500 m horizontal differences in $[NO_3^-]_{rem}/[PO_4^{3-}]_{rem}$ are

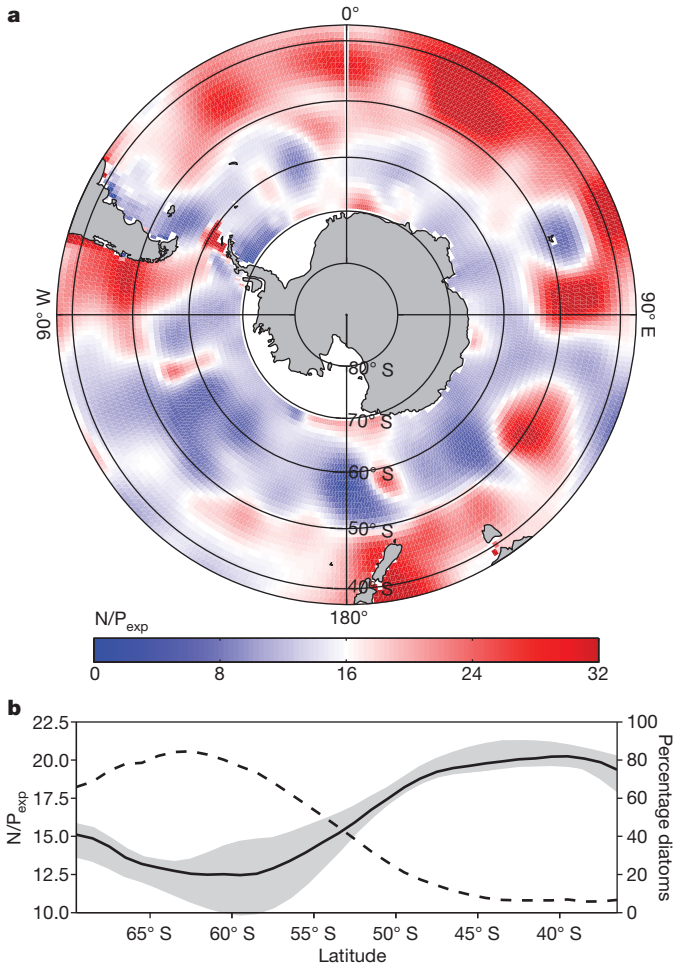

Figure 3 | Diagnosed nutrient export ratios. **a**, Spatial pattern of N/P_{exp}, derived in model 2 by diagnosing the export of NO_3^- and PO_4^{3-} independently. **b**, Zonal mean export ratio (solid line) and contribution of diatoms to N export (dashed line) diagnosed in model 2. The grey envelope is an estimate of errors associated with the choice of model compensation depth (50–100 m), the biological damping timescale (14 d to 1 yr) and the parameterization of dissolved organic matter (see Supplementary Information).

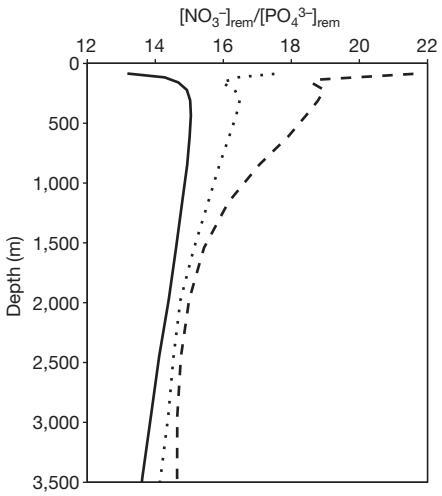

Figure 4 | Circulation averaging of remineralized nutrients. Depth profiles of $[NO_3^-]_{rem}/[PO_4^{3-}]_{rem}$ in the Antarctic (solid line), Polar frontal (dotted line) and sub-Antarctic (dashed line) zones predicted in model 3. The reduction in variability with depth results from the physical mixing of remineralized nutrients.

©2010 Macmillan Publishers Limited. All rights reserved

small and within the range detected from nutrient analyses in other basins[4]. The mixing of remineralized nutrients is sufficient to maintain the strong correlation ($R^2 = 0.99$) of NO_3^- and PO_4^{3-} in the subsurface, with a slope of N/P = 15.6:1 that is indistinguishable from the observed slope. Mixing is not strong enough, however, to entirely homogenize the remineralized nutrient ratios, and the small variations that remain bring the thermocline N* distribution into better agreement with the observations than in the Redfield prediction (Supplementary Fig. 6).

Whereas the hypothesis of ecosystem averaging cannot account for N* gradients in the surface of the Southern Ocean, circulation averaging is consistent with both surface and subsurface observations. The canonical covariation in NO_3^- and PO_4^{3-} in the deep ocean is thus maintained not by a uniform N/P ratio of nutrient assimilation and remineralization but by physical mixing across biogeographic provinces that are stoichiometrically very different.

Biogeochemical implications

Deviations from the Redfield N/P ratio on the scale of ocean biomes has broad implications for the understanding of nutrient limitation and the marine carbon cycle. The relationship between diatom production and community N/P ratio in the Southern Ocean is likely to exist throughout the surface ocean, although its detection from observations is confounded by exogenous inputs of fixed N and possibly a wider range of physiological acclimations on the global scale. In oligotrophic regions of the low-latitude ocean where $Si(OH)_4$ is scarce, this relationship implies a nutrient drawdown of ~20:1, consistent with the observed stoichiometry of sinking organic matter in the North Pacific Ocean[27]. This suggests that plankton communities of the subtropical ocean gyres may be more strongly N-limited than was previously recognized. The high metabolic N/P requirements in these biomes would expand the environmental selection for N_2 fixation by diazotrophs, which is in turn essential to sustaining the high N demand of the non-diazotrophic community. In this sense, the relationship between diazotrophs and other plankton may be more mutualistic than competitive. This helps resolve a previously noted paradox in the North Atlantic Ocean, where diazotrophs create a basin-scale excess of NO_3^- relative to a Redfield PO_4^{3-} quota but do not erase their ecological niche[28].

The stoichiometry of macronutrients also influences the amount of carbon sequestered in the deep ocean[7]. Because the cellular C/P ratios of plankton vary most strongly with N/P (ref. 9), the carbon export and air–sea CO_2 fluxes associated with a given degree of PO_4^{3-} drawdown depend on the balance of biomes with distinct N/P requirements. Recent evidence for reduced upwelling and opal production during the Last Glacial Maximum[29] suggests that diatoms were less prevalent in the glacial Southern Ocean. This would have increased the N/P ratio of nutrient removal, reconciling the apparent increase in NO_3^- use while PO_4^{3-} concentrations remained constant[30]. According to a simple three-box model of the oceanic carbon cycle[31], a 25% increase in high-latitude C/P ratios, reflecting an increase in N/P from 16:1 to 20:1, would reduce the concentration of atmospheric CO_2 by ~15 p.p.m. from interglacial levels. The predicted effects of contemporary climate warming on Southern Ocean upwelling[32] and the global distribution of marine biomes[33] could initiate perturbations in the marine nutrient and carbon cycles that cannot be anticipated by fixed-stoichiometry biogeochemical models.

METHODS SUMMARY

Model. We simulated the physical transport and biological cycling of nutrients in an ocean circulation model with a horizontal resolution of 1° and 23 vertical layers using the transport matrix method[34]. The geographic domain was split into two regions: an interior solution region (I), in which tracer distributions were simulated, and a boundary region (B), from which observed nutrient distributions[17] were transported into the interior. The conservation equations for nutrients (C stands for NO_3^- or PO_4^{3-}) and dissolved organic nutrients (C_{org} stands for dissolved organic N or P) are:

$$\frac{\partial C_I}{\partial t} = A_I C_I + A_B C_B - J_{ex} + J_{rem} - J_{org} + k_{org} C_{org,I} \quad (1)$$

$$\frac{\partial C_{org,I}}{\partial t} = A_I C_I + A_B C_{org,B} + J_{org} - k_{org} C_{org,I} \quad (2)$$

The A matrices represent physical transport processes within the interior region (A_I) and into the interior from the boundary (A_B). The J terms represent net biological nutrient removal from the surface (J_{ex}), remineralization in the subsurface (J_{rem}) and production of dissolved organic nutrients (J_{org}). C_{org} degrades by first-order decay at the rate k_{org}.

Simulations. We conducted three Southern Ocean simulations, in which annual mean nutrient distributions and fluxes were predicted by integrating equations (1) and (2) to the steady state. In model 1, the boundary was set at 35° S and PO_4^{3-} export was diagnosed by damping surface concentrations towards their observed values on a time scale τ_{damp}:

$$J_{ex}(C_I) = \max\left(\frac{C_I - C_{obs,I}}{\tau_{damp}}, 0\right) \quad (3)$$

NO_3^- export and remineralization were computed assuming a constant ratio of N/P = 16:1. In model 2, the Southern Ocean subsurface was incorporated into the boundary region, and the export of each nutrient was diagnosed independently using equation (3). Nutrient export by diatoms was estimated from diagnosed silicon fluxes and a simple model of the diatom Si/N ratio[23,35]. In model 3, the Southern Ocean subsurface was incorporated back into the solution region, and nutrient export and remineralization were simulated independently for N and P. See Supplementary Methods for further information.

Received 9 March; accepted 1 August 2010.

1. Redfield, A. C. The biological control of chemical factors in the environment. *Am. Sci.* **46,** 205–221 (1958).
2. Sterner, R. W. & Elser, J. J. *Ecological Stoichiometry: The Biology of Elements from Molecules to the Biosphere* 80–134 (Princeton Univ. Press, 2002).
3. Falkowski, P. G. Rationalizing elemental ratios in unicellular algae. *J. Phycol.* **36,** 3–6 (2000).
4. Anderson, L. A. & Sarmiento, J. L. Redfield ratios of remineralization determined by nutrient data analysis. *Glob. Biogeochem. Cycles* **8,** 65–80 (1994).
5. Takahashi, T., Broecker, W. S. & Langer, S. Redfield ratio based on chemical data from isopycnal surfaces. *J. Geophys. Res.* **90,** 6907–6924 (1985).
6. Codispoti, L. A. in *Productivity of the Ocean: Past and Present* (eds Berger, W. H., Smetacek, V. S. & Wefer, G.) 377–394 (Wiley, 1989).
7. Broecker, W. S. Glacial to interglacial changes in ocean chemistry. *Prog. Oceanogr.* **2,** 151–197 (1982).
8. Tyrrell, T. The relative influences of nitrogen and phosphorus on oceanic primary production. *Nature* **400,** 525–531 (1999).
9. Geider, R. J. & La Roche, J. Redfield revisited: variability of C:N:P in marine microalgae and its biochemical basis. *Eur. J. Phycol.* **37,** 1–17 (2002).
10. Quigg, A. *et al.* The evolutionary inheritance of elemental stoichiometry in marine phytoplankton. *Nature* **425,** 291–294 (2003).
11. Finkel, Z. V. *et al.* Irradiance and the elemental stoichiometry of marine phytoplankton. *Limnol. Oceanogr.* **51,** 2690–2701 (2006).
12. Klausmeier, C. A., Litchman, E., Daufresne, T. & Levin, S. A. Optimal nitrogen-to-phosphorus stoichiometry of phytoplankton. *Nature* **429,** 171–174 (2004).
13. Gruber, N. & Sarmiento, J. L. Global patterns of marine nitrogen fixation and denitrification. *Glob. Biogeochem. Cycles* **11,** 235–266 (1997).
14. Karl, D. M. & Michaels, A. F. in *Encyclopedia of Ocean Sciences* Vol. 4 (eds Steele, J. H., Turekian, K. K. & Thorpe, S. A.) 1876–1884 (Academic, 2001).
15. Dentener, F. *et al.* Nitrogen and sulfur deposition on regional and global scales: a multimodel evaluation. *Glob. Biogeochem. Cycles* **20,** GB4003 (2006).
16. Codispoti, L. A. & Christensen, J. P. Nitrification, denitrification, and nitrous oxide cycling in the eastern tropical Pacific Ocean. *Mar. Chem.* **16,** 277–300 (1985).
17. Garcia, H. E., Locarni, R. A., Boyer, T. P. & Antonov, J. I. *World Ocean Atlas 2005* Vol. 4 *Nutrients (Phosphate, Nitrate, Silicate)* (US Government Printing Office, 2006).
18. Orsi, A. H., Whitworth, T. W. & Nowlin, W. D. On the meridional extent and fronts of the Antarctic Circumpolar Current. *Deep-Sea Res. I* **42,** 641–673 (1995).
19. Schlitzer, R. Carbon export fluxes in the Southern Ocean: results from inverse modeling and comparison with satellite-based estimates. *Deep-Sea Res. II* **49,** 1623–1644 (2002).
20. Green, S. E. & Sambrotto, R. N. Plankton community structure and export of C, N, P and Si in the Antarctic Circumpolar Current. *Deep-Sea Res. II* **53,** 620–643 (2006).
21. Longhurst, A. Seasonal cycles of pelagic production and consumption. *Prog. Oceanogr.* **36,** 77–167 (1995).
22. Kopczynska, E. E., Weber, L. H. & El-Sayed, S. Z. Phytoplankton species composition and abundance in the Indian sector of the Antarctic Ocean. *Polar Biol.* **6,** 161–169 (1986).
23. Jin, X., Gruber, N., Dunne, J. P., Sarmiento, J. L. & Armstrong, R. A. Diagnosing the contribution of phytoplankton functional groups to the production and export of particulate organic carbon, $CaCO_3$, and opal from global nutrient and alkalinity distributions. *Glob. Biogeochem. Cycles* **20,** GB2015 (2006).
24. Price, N. M. The elemental stoichiometry and composition of an iron-limited diatom. *Limnol. Oceanogr.* **50,** 1159–1171 (2005).

©2010 Macmillan Publishers Limited. All rights reserved

25. Fu, F. X., Warner, M. E., Zhang, Y. H., Feng, Y. Y. & Hutchins, D. A. Effects of increased temperature and CO_2 on photosynthesis, growth, and elemental ratios in marine Synechococcus and Prochlorococcus (Cyanobacteria). *J. Phycol.* **43,** 485–496 (2007).
26. Arrigo, K. R. *et al.* Phytoplankton community structure and the drawdown of nutrients and CO_2 in the Southern Ocean. *Science* **283,** 365–367 (1999).
27. Karl, D. *et al.* The role of nitrogen fixation in biogeochemical cycling in the subtropical North Pacific Ocean. *Nature* **388,** 533–538 (1997).
28. Wu, J. F., Sunda, W., Boyle, E. A. & Karl, D. M. Phosphate depletion in the western North Atlantic Ocean. *Science* **289,** 759–762 (2000).
29. Anderson, R. F. *et al.* Wind-driven upwelling in the Southern Ocean and the deglacial rise in atmospheric CO_2. *Science* **323,** 1443–1448 (2009).
30. Elderfield, H. & Rickaby, R. E. M. Oceanic Cd/P ratio and nutrient utilization in the glacial Southern Ocean. *Nature* **405,** 305–310 (2000).
31. Sarmiento, J. L. & Toggweiler, J. R. A new model for the role of the oceans in determining atmospheric PCO_2. *Nature* **308,** 621–624 (1984).
32. Le Quere, C. *et al.* Saturation of the Southern Ocean CO_2 sink due to recent climate change. *Science* **316,** 1735–1738 (2007).
33. Sarmiento, J. L. *et al.* Response of ocean ecosystems to climate warming. *Glob. Biogeochem. Cycles* **18,** GB3003 (2004).
34. Khatiwala, S., Visbeck, M. & Cane, M. A. Accelerated simulation of passive tracers in ocean circulation models. *Ocean Model.* **9,** 51–69 (2005).
35. Brzezinski, M. A. *et al.* A switch from $Si(OH)_4$ to NO_3^- depletion in the glacial Southern Ocean. *Geophys. Res. Lett.* **29,** 1564 (2002).

Supplementary Information is linked to the online version of the paper at www.nature.com/nature.

Acknowledgements We thank S. Khatiwala for providing the transport matrix. This work was funded by grants from the National Science Foundation and the Gordon and Betty Moore Foundation. Additional support for T.S.W. was provided by a Pauley Fellowship from UCLA.

Author Contributions T.S.W. conducted the simulations and analysed the results. C.D. designed the study. Both authors wrote the paper.

Author Information Reprints and permissions information is available at www.nature.com/reprints. The authors declare no competing financial interests. Readers are welcome to comment on the online version of this article at www.nature.com/nature. Correspondence and requests for materials should be addressed to T.S.W. (tweber@atmos.ucla.edu).

©2010 Macmillan Publishers Limited. All rights reserved